J|A|C|S COMMUNICATIONS

Published on Web 04/08/2009

Solar Water Oxidation by Composite Catalyst/α-Fe_2O_3 Photoanodes

Diane K. Zhong, Jianwei Sun, Hiroki Inumaru, and Daniel R. Gamelin*

Department of Chemistry, University of Washington, Seattle, Washington 98195-1700

Received March 3, 2009; E-mail: Gamelin@chem.washington.edu

The photoelectrochemical (PEC) conversion of photon power into chemical fuels offers an attractive approach to storing solar energy,[1,2] but it poses many fundamental chemical challenges. Hematite (α-Fe_2O_3) has emerged as a prototype photoanode material for testing strategies to overcome the challenging four-electron oxidation of water,[2] which under basic conditions is described by eq 1.

$$4OH^- \rightarrow O_2 + 4e^- + 2H_2O \quad (1)$$

Hematite meets many of the target photoanode requirements: It is inexpensive, oxidatively robust, environmentally benign, and absorbs visible light (E_g ~2.1 eV). Although the α-Fe_2O_3 valence band edge potential is >1 V more negative than required for eq 1 thermodynamically, water oxidation by photogenerated valence-band holes in α-Fe_2O_3 is kinetically inefficient, and additional anodic overpotentials are typically required before significant PEC water splitting is observed. A remaining fundamental limitation of α-Fe_2O_3 is that its conduction band edge potential resides ~200 mV below that required to drive the cathodic half-reaction (eq 2).

$$2H_2O + 2e^- \rightarrow H_2 + 2OH^- \quad (2)$$

Tandem PEC/photovoltaic (PV) configurations have been envisioned to provide the bias needed to meet these demands.[3] Recent advances in controlled growth and doping of α-Fe_2O_3 nanostructures[2−6] have overcome many of the limitations associated with the short hole-diffusion length (~2−4 nm), low electron mobility (~10^{-1} cm^2 V^{-1} s^{-1}), and efficient charge carrier recombination characteristics of bulk α-Fe_2O_3, yielding promising PEC performance. For example, an overall solar-to-hydrogen power conversion efficiency of ~2.1% has been estimated for one set of mesostructured α-Fe_2O_3 photoanodes when powered by a PV device providing 1.4 V in a tandem configuration.[3b] Unfortunately, many low-cost PV devices such as dye-sensitized solar cells or organic PVs typically provide <1 V, and two such PVs in series would thus be required to provide the necessary 1.4 V. The development of α-Fe_2O_3 photoanodes that require smaller overpotentials to oxidize water, such that they could be powered by single low-cost PV cells, would thus be attractive for reducing solar hydrogen production costs.

Recently, electrochemical water oxidation with low overpotentials was demonstrated over a range of pH values using an amorphous cobalt/phosphate catalyst ("Co-Pi") electrodeposited onto ITO or FTO electrodes.[7] Remaining uncertainties about the catalyst's precise microscopic identity do not diminish its attractiveness for water-splitting PECs. Co-Pi requires only a 0.41 V overpotential at pH 7 to oxidize water with a current density of 1 mA/cm^2,[7a] whereas the α-Fe_2O_3 valence band edge potential provides >~1.2 V. Photogenerated holes in α-Fe_2O_3 should thus be amply capable of driving water oxidation by this electrocatalyst. Here we report that composite photoanodes made by electrodeposition of Co-Pi onto mesostructured α-Fe_2O_3 show >350 mV cathodic shifts of the onset potential for PEC water oxidation while retaining substantial photocurrent densities.

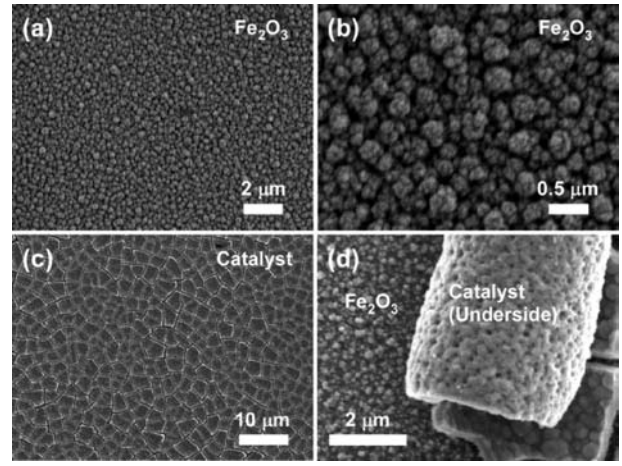

Figure 1. SEM images of mesostructured α-Fe_2O_3 photoanode before (a,b) and after (c,d) electrodeposition of Co-Pi catalyst. The catalyst layer cracking occurs upon drying for the SEM measurement and in some cases allows inspection of the catalyst underside: Panel (d) shows that the Co-Pi underside topology conforms to the α-Fe_2O_3 mesostructure.

Following previous reports,[3b−d] mesostructured Si-doped α-Fe_2O_3 photoanodes of 400−500 nm thickness were grown by atmospheric pressure chemical vapor deposition (APCVD) using $Fe(CO)_5$ and TEOS as precursors, delivered to an FTO substrate at 470 °C using Ar carrier gas. SEM images of a representative α-Fe_2O_3 photoanode are shown in Figure 1a,b and reveal a highly structured electrode surface. PEC measurements were then performed in a three-electrode configuration using an aqueous OH^- electrolyte (1 M NaOH, pH 13.6), a Pt counter electrode, and Ag/AgCl as the reference electrode. Photocurrent densities were measured as a function of applied voltage under simulated 1 sun AM1.5 solar irradiation (see Supporting Information (SI)). As in previous studies, the α-Fe_2O_3 PEC performance was found to depend strongly on surface morphology, Si doping level, and growth temperature, among other parameters.[3]

Figure 2a shows dark and photocurrent densities for an α-Fe_2O_3 photoanode with backside illumination. Whereas the dark response is negligible up to 1.5 V vs RHE, the photoresponse shows a rise and plateau with an onset voltage of ~1 V vs RHE that typifies α-Fe_2O_3. Figure 1c,d show SEM images of a representative α-Fe_2O_3 photoanode following Co-Pi electrodeposition for 1 h as described in ref 7 (see SI). Extensive cracking of the ~200 nm thick catalyst layer occurs upon drying for the SEM measurement. Figure 1d shows a portion of the catalyst layer that has curled off of the α-Fe_2O_3 film upon drying, revealing its underside. This image shows the inverse mesostructure from the α-Fe_2O_3 anode, demonstrating that the catalyst layer conforms to the topology of the α-Fe_2O_3 surface. A high degree of interfacial contact between the α-Fe_2O_3 and catalyst layers has thus been achieved. Figure 2a also shows the dark and photocurrent responses of the Co-Pi/α-Fe_2O_3 composite photoanode prepared by electrodeposition of the Co-Pi catalyst on

10.1021/ja9016478 CCC: $40.75

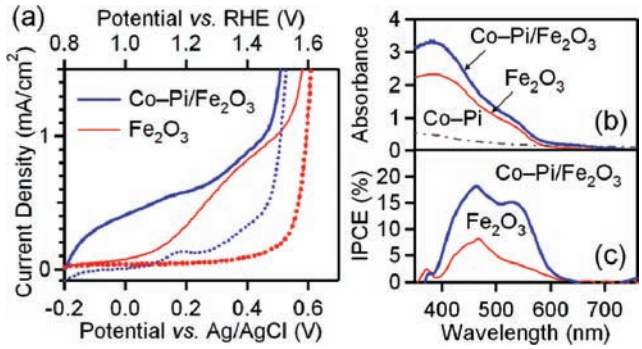

Figure 2. (a) Dark (dashed) and photocurrent (solid) densities for α-Fe_2O_3 (red) and Co-Pi/α-Fe_2O_3 (blue) photoanodes, collected using simulated AM1.5 illumination (1 sun, backside) at a scan rate of 50 mV/s. (b) Electronic absorption and (c) IPCE spectra for α-Fe_2O_3 and Co-Pi/α-Fe_2O_3 (at 1.23 and 1 V vs RHE, respectively). The absorption spectrum of Co-Pi on FTO without α-Fe_2O_3 is included in (b), but no photocurrent was detected for these anodes.

the same α-Fe_2O_3 photoanode. The major phenomenological observation is that modification of α-Fe_2O_3 with Co-Pi reduces the bias voltage required for solar PEC water oxidation by >350 mV, corresponding to a reduction from ∼1.2 to <∼0.9 V that would be required from the PV of a water splitting PEC/PV tandem cell.

At 1.4 V (RHE), α-Fe_2O_3 photocurrent densities with front-side illumination are ∼2× greater than those with backside illumination (see SI), a common observation[3b−d] attributable to the greater surface area of the anode front. In the Co-Pi/α-Fe_2O_3 anodes, however, front-side illumination did not greatly enhance the photocurrent, likely because of nonproductive absorption by the catalyst layer. Co-Pi absorbs throughout the visible spectral region (Figure 2b) but generates no detectable photocurrent, either on α-Fe_2O_3 or directly on FTO. IPCE measurements of the α-Fe_2O_3 (1.23 V vs RHE) and Co-Pi/α-Fe_2O_3 (1 V vs RHE) photoanodes using backside illumination show essentially identical dispersion (Figure 2c), in both cases apparently deriving only from α-Fe_2O_3 excitation. Co-Pi thus behaves solely as a surface electrocatalyst. The composite photoanode of Figure 2c shows IPCE > 15% at 550 nm and 1 V vs RHE, conditions where α-Fe_2O_3 alone shows negligible photocurrent (Figure 2a). This IPCE maximizes at 450 nm (18%) before decreasing again below ∼400 nm because of the decreasing light penetration depth (Figure 2b).

Several control experiments were performed to test the possibility that the cathodic photocurrent shift might derive from unintended side reactions. The possibility of dissolved cobalt acting as a redox mediator, or of an unidentified sacrificial reagent contributing to photocurrent, was eliminated by the following observations: (i) Addition of solvated Co^{2+} to the electrolyte had no noticeable effect on photocurrent densities (see SI); (ii) Replacement of the PEC electrolyte solution with new stock solution caused no change in photocurrent and did not lead to a photocurrent induction period; (iii) Continuous photocatalysis at 1 V vs RHE for >10 h showed no change in performance. We conclude that the cathodic shift in Figure 2 reflects the ability to drive eq 1 at much smaller overpotentials using the composite photoanodes than with α-Fe_2O_3 alone.

Most α-Fe_2O_3 PEC cells operating under similar conditions show negligible photocurrent densities below 1 V vs RHE. Modification of the α-Fe_2O_3 surface by adsorption of Co^{2+} from aqueous 10 mM $Co(NO_3)_2$ was previously shown to cause an ∼17% increase in current density at 1.23 V vs RHE and an 80 mV cathodic shift of the onset potential.[3c] Similarly, growth of RuO_2 onto α-Fe_2O_3 surfaces led to a 120 mV cathodic shift of the onset potential with <80 $\mu A/cm^2$ at 1 V vs RHE.[4b] Interestingly, α-Fe_2O_3 nanorods have shown greater relative

Scheme 1

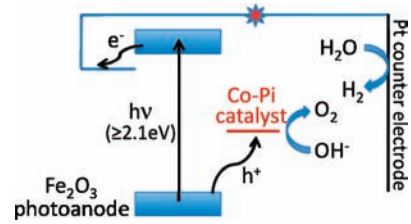

photocurrent densities at low bias than typical mesostructured α-Fe_2O_3 photoanodes, but with photocurrent densities of only ∼2 $\mu A/cm^2$.[6] We hypothesize that the conformal catalyst deposition facilitates interfacial hole transfer from α-Fe_2O_3 to Co-Pi, allowing photon absorption and redox catalysis to be effectively decoupled while retaining photocurrent densities. Efficient hole transfer from α-Fe_2O_3 to Co-Pi should enhance the electron gradient in the α-Fe_2O_3 mesostructure under irradiation, also contributing to the driving force for electron diffusion to the FTO and reducing deleterious carrier recombination processes. Catalyst electrodeposition onto α-Fe_2O_3 may also passivate surface defects.

The experimental results for the Co-Pi/α-Fe_2O_3 composite photoanodes are summarized in Scheme 1. Photoexcitation of α-Fe_2O_3 generates an electron−hole pair. Photogenerated holes are trapped by the Co-Pi catalyst, which excels at water oxidation. Photogenerated electrons migrate to the FTO back contact and pass through the circuit to the Pt counter electrode, where water reduction occurs in the three-electrode configuration. The present results demonstrate that partitioning photoabsorption, charge separation, and redox catalysis in composite photoanodes offer promising opportunities for improving solar water-splitting PECs. A complete microscopic understanding of these composite photoanodes will require a better understanding of the Co-Pi/α-Fe_2O_3 interface and of hole transfer across this interface. Experiments to address these issues are presently underway.

Acknowledgment. This work was funded by the Dreyfus Foundation, ACS-PRF (AC), the NSF (IGERT, DGE-050-4573), the University of Washington, the UW Initiative Fund (UIF), and was partially conducted at the UW Nanotechnology User Facility, a member of NNIN. The authors thank Dr. K. Sivula, Prof. S. Adler, and Prof. M. Grätzel for stimulating discussions.

Supporting Information Available: Experimental details, α-Fe_2O_3 front vs backside photocurrent data, and $Co(OH)_4^{2-}$ absorption spectrum. This information is available free of charge via the Internet at http://pubs.acs.org.

References

(1) (a) Heller, A. *Science* **1984**, *223*, 1141. (b) Grätzel, M. *Nature (London)* **2001**, *414*, 338. (c) Lewis, N. S.; Nocera, D. G. *Proc. Natl. Acad. Sci. U.S.A.* **2006**, *103*, 15729. (d) Lewis, N. S. *Science* **2007**, *315*, 798.
(2) (a) Grimes, C.; Varghese, O. K.; Ranjan, S. *Light, Water, Hydrogen*; Springer: 2007. (b) van de Krol, R.; Liang, Y.; Schoonman, J. *J. Mater. Chem.* **2008**, *18*, 2311.
(3) (a) Duret, A.; Grätzel, M. *J. Phys. Chem. B* **2005**, *109*, 17184. (b) Cesar, I.; Kay, A.; Gonzalez Martinez, J. A.; Grätzel, M. *J. Am. Chem. Soc.* **2006**, *128*, 4582. (c) Kay, A.; Cesar, I.; Grätzel, M. *J. Am. Chem. Soc.* **2006**, *128*, 15714. (d) Cesar, I.; Sivula, K.; Kay, A.; Zboril, R.; Grätzel, M. *J. Phys. Chem. C* **2009**, *113*, 772.
(4) (a) Ingler, W. B.; Khan, S. U. M. *Electrochem. Solid-State Lett.* **2006**, *9*, G144. (b) Majumder, S. A.; Khan, S. U. M. *Int. J. Hydrogen Energy* **1994**, *19*, 881.
(5) Kleiman-Shwarsctein, A.; Hu, Y.-S.; Forman, A. J.; Stucky, G. D.; McFarland, E. W. *J. Phys. Chem. C* **2008**, *112*, 15900.
(6) Lindgren, T.; Wang, H.; Beerman, N.; Vayssieres, L.; Hagfeldt, A.; Lindquist, S.-E. *Sol. Energy Mat. Sol. Cells* **2002**, *71*, 231.
(7) (a) Kanan, M. W.; Nocera, D. G. *Science* **2008**, *321*, 1072. (b) Surendranath, Y.; Dincă, M.; Nocera, D. G. *J. Am. Chem. Soc.* **2009**, *131*, 2615. (c) Lutterman, D. A.; Surendranath, Y.; Nocera, D. G. *J. Am. Chem. Soc.* **2009**, *131*, 3838.

JA9016478